Phonons in liquid ^{4}He from a heated metal film. I. The creation of high-frequency phonons

1994 J. Phys.: Condens. Matter 6 2813

(http://iopscience.iop.org/0953-8984/6/15/004)

J. Phys.: Condens. Matter 6 (1994) 2813–2824. Printed in the UK

Phonons in liquid ^{4}He from a heated metal film: I. The creation of high-frequency phonons

M A H Tucker and A F G Wyatt
Department of Physics, University of Exeter, Stocker Road, Exeter EX4 4QL, UK

Received 15 December 1993, in final form 24 January 1994

Abstract. For a very short ($t_p < 0.25$ μs) Joule heating pulse in a metal film heater submerged in liquid ^{4}He at low temperatures ($T < 0.1$ K), the phonons created in the liquid separate into distinct low-frequency and high-frequency distributions. Phonons of intermediate frequencies are absent from the signal because they spontaneously decay to lower frequencies. High-frequency phonons above the decay cut-off ($\omega > \omega_c^{(\infty)}$) are stable as $T \to 0$. We find that for a heater power of 10 mW mm^{-2}, these high-frequency phonons are not distributed over the available frequency range up to the maxon, but are concentrated in a narrow band around $\omega_c^{(\infty)}$. Times of flight show that the distribution of high-frequency phonons depends upon pressure P such that the peak is always at the pressure dependent decay cut-off $\omega_c^{(\infty)}(P)$. We suggest that the majority of these detected high-frequency phonons is produced in the liquid ^{4}He by frequency up scattering processes amongst the injected phonons.

1. Introduction

Liquid ^{4}He is an ideal medium in which to study phonon propagation because there are no defects as in solids, only longitudinal phonons are present, and it is isotropic. The only impurities are ^{3}He atoms, which can be reduced to abundance levels of less than 1 part in 10^{12} [1]. Phonons in liquid ^{4}He can be studied by creating them with a pulsed heater and measuring the energy flux as a function of time of flight over a propagation path length. Once the phonons have been created, they can spontaneously decay or be scattered by interactions with other phonons. Good progress in understanding the propagation of phonons has been made [2], but less is known about the phonon creation processes at the liquid boundary [3, 4]. In this pair of papers, we report on our experimental investigations into the creation of phonons in liquid ^{4}He when a metal film is heated by a current pulse.

The dispersion of phonons in liquid ^{4}He has an upward (positive) curvature at low frequencies [5–8] and negative curvature at higher frequencies. This allows phonons with $\omega < \omega_c^{(\infty)}$ to spontaneously decay into numerous low-frequency phonons, while phonons with $\omega > \omega_c^{(\infty)}$ are stable against such decays [2]. At the saturated vapour pressure (SVP), $\hbar\omega_c^{(\infty)}/k_B = 10$ K [9] from neutron scattering data [10]. The positive curvature decreases with increasing pressure P [11–14], such that $\omega_c^{(\infty)}$ decreases from its maximum value at SVP to zero at $P \simeq 19$ bar [15]. For $P > 19$ bar, the dispersion has negative curvature for all phonon frequencies so no decays are permitted.

The decay cut-offs $\omega_c^{(n)}$ depend upon n, the number of phonons produced in the decay. At SVP, the three-phonon ($p_1 \to p_2 + p_3$) decay cut-off is $\hbar\omega_c^{(2)}/k_B \simeq 8.5$ K [9], estimated from neutron scattering data [10] of the dispersion curve. The theoretical rate for the three-phonon process (3PP) has been calculated [16, 17]. For $\omega < \omega_c^{(2)}$, the decay rate is

0953-8984/94/152813+12$19.50

$7.12 \times 10^5 \varepsilon^5$ s^{-1}, where ε is the energy in units of kelvin of the initial phonon [2]. For a 7.5 K phonon, this corresponds to a mean free path of ~ 140 Å.

Neutron spin echo techniques measure the neutron scattering line widths to give phonon lifetimes. This gives a mean free path of $\sim 530 \pm 170$ Å for 7.5 K phonons [18]. Some of the discrepancy between theory and experiment may be due to the dispersion curve parameterization used in the calculation of the decay rates. There is, as yet, no experimental confirmation that the 3PP decay rate in liquid ^{4}He is actually proportional to ε^5.

Phonons with $\omega < \omega_c^{(\infty)}$ can spontaneously decay into many low-frequency phonons, but these decay rates are expected to be slower than the 3PP due to the smaller terms in the perturbation expansion of the Hamiltonian and to momentum space available for final states, although they have not yet been calculated [2]. The cut-offs $\omega_c^{(n)}$ increase with greater n towards the limit of $\hbar\omega_c^{(\infty)}/k_B = 10$ K. Consequently, for finite path lengths, the decay cut-off measured from the propagation of phonons between a source and a detector will be below $\omega_c^{(\infty)}$. The decay cut-off for phonons in liquid ^{4}He, travelling over a path length of 1.1 mm, is $\hbar\omega_c/k_B \simeq (9.80 \pm 0.15)$ K at SVP [15, 19].

So, at low temperatures and pressures, the phonon spectrum is composed of two distributions due to these spontaneous decays [9]. The distribution of phonons with low frequencies will have $\hbar\omega/k_B \leqslant 1$ K because the phonons continue to decay until the mean free path becomes comparable with the remaining path length. These low-frequency phonons travel at the ultrasonic velocity. The other distribution will comprise phonons with frequencies $\omega > \omega_c^{(n)}$, where n is determined by the spontaneous decay rates and the signal path length. These high-frequency phonons can travel ballistically at group velocities

$$v_g \leqslant (\partial\omega/\partial q)|_{\omega_c^{(n)}} \tag{1}$$

because at sufficiently low temperatures ($T < 0.1$ K), the mean free paths of the high-frequency phonons in liquid ^{4}He between interactions with ambient thermal phonons are greater than the sample dimension of a few centimetres [20]. For a phonon pulse injected into the liquid by a heater, the size of the high-frequency phonon signal relative to the low-frequency phonon signal can be estimated. The two signals are separated by velocity dispersion.

The partition of energy between the two phonon distributions is very unequal if they arise from a thermal source. There is much more energy in the low-frequency phonon group, because these phonons are in the dominant background channel, where phonons are produced by energy down conversion at the heater/^{4}He interface [4]. The effective temperature of these phonons is ~ 0.7 K [21]. There are also phonons that are transmitted across this interface via the elastic channel (frequency conserved) [22]. The distribution of these has a higher effective temperature of about 2 K (the heater temperature [23]). The ratio of elastic channel to background phonons has been estimated at 5×10^{-3} for a metal surface [9]. So the energy fraction in $\omega > \omega_c^{(\infty)}$ phonons is $\sim 5.5 \times 10^{-3}$ of the total energy.

Indications of the relative signal sizes can be obtained from previous measurements of $\alpha(\omega)$, the frequency dependent transmission coefficient of phonons between the liquid and a solid [3, 24, 25]. Using these parameters, the high-frequency phonon signal should be barely detectable using a bolometer in the liquid [26]. However, we will show that by a judicious choice of heater power and pulse duration, we can increase the relative size of the high-frequency phonon signal. This makes it possible to clearly detect the high-frequency phonons from a metal film heater using a bolometer submerged in the liquid. Being able to detect these high-frequency phonons, we can investigate how they are created in the liquid ^{4}He by a metal film heater.

The spectrum of phonons in a heater is distinctly non-Planckian, and is weighted towards higher frequencies due to the electron–phonon coupling [27, 28]. The transmission probability of phonons across the heater/liquid ^{4}He interface is dependent upon phonon frequency [3], so the phonon spectrum in the liquid is not identical to the phonon spectrum in the heater. All the experimental evidence so far put forward has indicated that the phonons injected into liquid ^{4}He can be described by a Planck distribution [25, 9]. This is probably because the dominant transmission channel is inelastic, involving the emission of down converted phonons from surface states [9].

Experiments have shown that the spectrum of phonons created in the liquid depends upon the power density in the heater [9, 29]. The spectrum was deduced from the signal measured at a superconducting tunnel junction (STJ) detector positioned several millimetres from the heater. Three power regimes were identified for 1 μs pulses: low (< 5 mW mm^{-2}), medium (5–20 mW mm^{-2}), and high (> 20 mW mm^{-2}). At low powers, the measurements indicated that the spectrum of phonons above the decay cut-off can be represented by the high-frequency tail of a Planck distribution. Phonons below the cut-off decay to lower frequencies. At medium powers, the beam interactions appear to destroy as many high-frequency phonons as they create, thus giving a plateau in a $\omega > \omega_c^{(\infty)}$ signal versus power plot. At high powers, the beam interactions are so numerous that the phonons in the pulse are completely non-ballistic, and these interactions give a fast rise in the $\omega > \omega_c^{(\infty)}$ signal versus power plot.

The boundaries between these power regimes are probably affected by the heater pulse length. This is because the production of high-frequency phonons is critically dependent upon pulse length t_p. For $t_p > 0.25$ μs, the high-frequency ($\omega > \omega_c^{(\infty)}$) phonon signal saturates [30, 31], whereas low-frequency phonons are produced at an almost constant rate for all pulse lengths [30].

Experiments using very long pulse lengths, typically $t_p = 300$ μs, have indicated that a layer of liquid ^{4}He close to the heater surface can act as an intermediate stage in the phonon transmission from the solid to the liquid [32, 33]. By assuming black body radiation of phonons from the surface of this layer into the bulk liquid, it was inferred that the shape and extent of this layer changes with heater power. These experiments were performed using C film heaters. This behaviour is not thought to occur for $t_p < 10$ μs.

So, the investigation of phonon creation in liquid ^{4}He by a heater is complicated by transmission processes at the interface and by scattering processes in the liquid. The importance of these processes appears to depend upon both heater power and pulse length.

In this paper, we present our measurements of the high-frequency phonon spectrum created by heaters of various metals, the change in signal velocity with hydrostatic pressure, and the progressive attenuation of this signal with increasing liquid ^{4}He temperature. We use a medium heater power density (10 mW mm^{-2}) to give a clearly detectable high-frequency phonon signal, and a very short pulse ($t_p \leqslant 0.2$ μs) to ensure that the high-frequency phonon production has not saturated. We find that for short pulses of medium power, the high-frequency phonons are predominantly created by interactions in the liquid close to the heater. In the subsequent companion paper [26], we measure the angular distribution of phonons emitted by an Au film heater and show how important this aspect is for our ability to detect the high-frequency phonons.

2. Experiment

The experimental apparatus consists of a heater and a bolometer directly facing each other at a separation of 15.7 ± 0.1 mm. The heater is a 1 mm $\times$ 1 mm metal film evaporated

onto a glass microscope cover slide, and has a resistance of about 50 Ω. Most of the results in this paper were obtained using various Au film heaters. Trials with a Cr film heater and a non-superconducting Ti film heater [34] have also given similar results, so the metal composition of the heater seems to be relatively unimportant. The bolometer is a Zn film evaporated onto a glass cover slide, with a resistance of a few ohms per square at room temperature. The zinc is scratched with interleaved lines to give a serpentine path for the electrical current and a resistance at room temperature of several hundred ohms. The detecting area of the Zn bolometer is 1 mm × 1 mm.

The experiment is situated inside a brass cell, which is cooled by a dilution refrigerator to a base temperature of ~ 60 mK. The temperature was measured using the resistance of an RuO chip placed inside the cell. This chip had previously been calibrated against a commercially calibrated Ge thermometer [35]. Purified ^{4}He [36] is condensed into the cell until both the heater and bolometer are submerged to give a direct liquid path between them. The heater is Joule heated by a short (~ 0.1 μs) electrical pulse to create excitations in the liquid ^{4}He. These excitations are detected upon reaching the bolometer. The signals are independent of collimation configurations, i.e. echoes caused by excitations reflected from surfaces inside the experimental cell are not observed. In this paper, the results were obtained both with and without collimation.

The detection system operates on the constant-temperature bolometer principle [37]. The bolometer is operated on its transition edge at about half its normal resistance at low temperatures. By applying a magnetic field parallel to the Zn surface, the transition temperature is reduced to ~ 0.3 K, which enables low temperatures in the cell to be achieved. The bolometer is kept at this temperature by the Joule heating due to the bias current from a feedback amplifier. When a phonon flux arrives at the bolometer, the accepted energy is balanced by a reduction in the feedback to maintain the temperature of the Zn at its steady state value. The variation in feedback, which is directly proportional to the accepted energy flux, is amplified and stored as a digitized waveform on a Biomation 8100. Because of the very small signals involved, averages of $64k$, where $k = 1024$, are often required for each waveform to increase the signal to noise ratio. The time constant of the detection system is < 1 μs.

The analysis of evaporation signals from liquid ^{4}He has shown that the high-frequency phonon signal saturates for heater pulse lengths $t_p > 0.25$ μs at a power W of 10 mW mm^{-2} [30]. So, in this investigation, $t_p = 0.1$ μs and $W = 10$ mW mm^{-2} unless specified otherwise. Pulses of this duration and power seem to optimize the high-frequency phonon production relative to both low-frequency phonons and rotons [30]. Any rotons created by the heater are unlikely to be detected because the transmission probability of their energy into a Zn bolometer is much less than that for phonons.

3. Results and discussion

At low pressures, the detected signal from a 0.1 μs, 10 mW pulse contains two peaks separated in time as shown in figure 1. At SVP, the arrival time of the first peak corresponds to a signal velocity of 238 m s^{-1}, and it is therefore identified with the low-frequency phonons. The peak is narrow because there is little dispersion. The second peak is superimposed upon the tail from the first peak. This tail is probably due to the emission of low-frequency phonons from the cooling glass substrate beneath the metal film heater. The arrival time of the maximum of the second peak corresponds with a velocity of ~ 187 m s^{-1}, which is equal to the gradient of the dispersion curve, as measured by neutron scattering

[13], for $\hbar\omega/k_B \simeq 10.15$ K phonons. This is only slightly above the threshold of stability against spontaneous decay at 10 K. If we assume that the high-frequency phonons travel from the heater to the bolometer without changes in velocity due to interactions, then this second peak is due to the detection of $\omega \simeq \omega_c^{(\infty)}$ phonons. The gap between the two peaks is due to spontaneous phonon decays.

In this paper, we will first show that the second peak in the signals is indeed due to high-frequency phonons (section 3.1). In section 3.2, we obtain the spectrum of high-frequency phonons directly from the signal shape by assuming that the phonons are created at the heater surface and travel ballistically to the detector. This is done to illustrate how much the phonon spectrum differs from the Planck spectrum found for longer pulse lengths and lower powers [29].

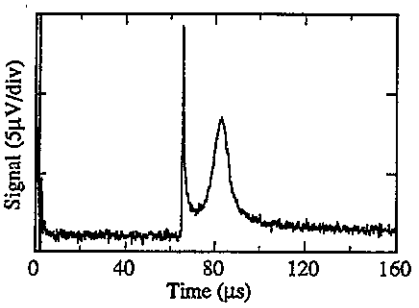

Figure 1. The signal from a 0.1 μs, 10 mW mm^{-2} heater pulse that has travelled through 15.7 mm of liquid ^{4}He at $T < 0.1$ K and at SVP. The large signal at small times ($t < 5$ μs) is due to the electrical pick-up of the heater pulse by the wires to the bolometer.

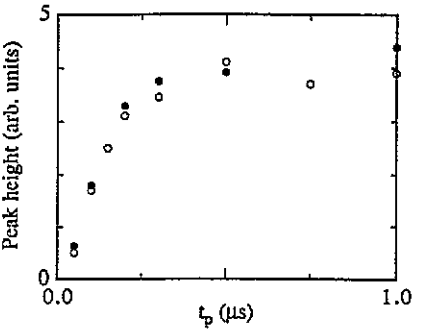

Figure 2. The peak signal height as a function of heater pulse length t_p at SVP and $t < 0.1$ K. Open symbols (○) are for evaporation signals at normal incidence to the liquid surface, closed symbols (●) for signals that have travelled entirely through the liquid. The heater power is 5 mW mm^{-2}.

The variation of this second peak with pressure (section 3.3) yields information on the phonon creation processes, and leads to the important conclusion that the high-frequency phonons are created by scattering processes amongst lower-frequency phonons in the liquid (section 3.4). In section 3.5, we show that this is consistent with the time of flight anomaly observed in phonon evaporation signals [31, 38, 39]. Finally, in section 3.6 we show that the attenuation of the second peak with liquid ^{4}He temperature is consistent with the thermal attenuation of the phonon quantum evaporation signals. This gives further confidence that the second peak is the detection of high-frequency phonons.

3.1. Pulse width dependence

One signature of high-frequency phonons signals is their dependence upon heater pulse width. Quantum evaporation experiments have shown that the signal from high-frequency phonons saturates after $t_p = 0.25$ μs for $W = 10$ mW mm^{-2} [30, 31]. This behaviour distinguishes high-frequency phonons from low-frequency phonons and rotons, both of which give signals that increase almost linearly with pulse width. Therefore, important evidence for the attribution of the second peak to high-frequency phonons is its magnitude as a function of pulse duration t_p. The magnitude of the second peak as a function of t_p is shown in figure 2, together with some results from phonon evaporation signals. The

similarity between the two sets of measurements is convincing evidence that the second peak is due to high-frequency phonons.

This dependence upon pulse width therefore explains why these twin-peaked signals have not been observed before with bolometers in the liquid. Most of the previous experiments on phonon emission and propagation in liquid ^{4}He were carried out using $t_p \geqslant 1$ μs. Our data show that for $t_p > 1$ μs, the tail of the first peak is so large that the second peak becomes unnoticeable. An example, for a 5 μs pulse, is shown in figure 3. Some experiments using STJ detectors have given signals with two distinct components because STJ detectors do not detect the low-frequency ($\hbar\omega < 2\Delta$) phonons and so the high-frequency phonon signal is not swamped [9].

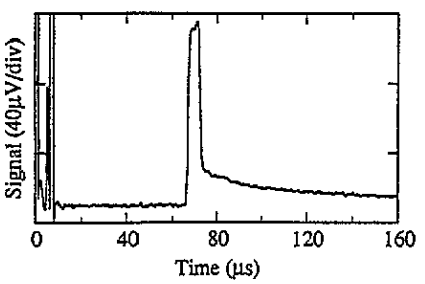

Figure 3. The signal from a 5 μs, 5 mW mm^{-2} heater pulse that has travelled through 15.7 mm of liquid ^{4}He at $T < 0.1$ K and at SVP.

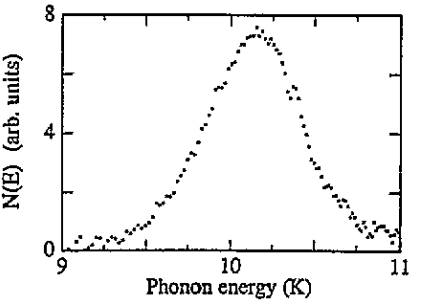

Figure 4. A first estimate of the spectrum of high-frequency phonons (energy expressed in units of kelvin) created in liquid ^{4}He by a metal film heater. The spectrum was obtained from the signal shown in figure 1, on the assumption that the phonons travel ballistically from the heater surface to the bolometer. The true spectrum of phonons arriving at the detector is probably narrower than this due to the creation processes described later.

3.2. An estimate of the high-frequency phonon spectrum

The spectrum of high-frequency phonons in the signal's second peak (figure 1) can be obtained from its temporal shape using a parameterized dispersion curve [20] fitted to neutron scattering data [13]. When submerged in the liquid ^{4}He, the time constant of the bolometer is limited to the electrical feedback response of < 1 μs. The sampling rate of the Biomation is 0.1 μs. So the signal shape will yield reasonably accurate information about the spectrum of phonons arriving at the bolometer, as long as they are created at the heater surface and thereafter travel ballistically. We return to this point at the end of this section. Assuming that the phonons are ballistic between the heater surface and the bolometer surface, then the spectrum appears to be centred upon $\hbar\omega/k_B = (10.15 \pm 0.10)$ K with a half width at half maximum of $\hbar\Delta\omega/k_B \simeq 0.35$ K, as shown in figure 4.

Previous work at low and medium heater power densities has assumed that the high-frequency phonons have a broad distribution of energies that can be represented by the high-energy tail of a Planck spectrum [9]. While this is so at low powers (< 2 mW mm^{-2}), we see that this is certainly not the case for this medium power (10 mW mm^{-2}) and short pulse duration. Rather than the broad spectrum of phonons in the tail of a Planck spectrum,

there is a narrow spectrum with a maximum at approximately the decay cut-off $\omega_c^{(\infty)}$. We find that this is true for powers $\geqslant 2$ mW mm^{-2}, up to at least 40 mW mm^{-2}. 2 mW mm^{-2} is the low-power threshold for obtaining an observable high-frequency phonon signal with a bolometer in the liquid. For lower powers it is likely that the high-frequency phonon distribution is closer to a Planck spectrum, but with the present experimental arrangement involving a bolometer rather than an STJ, the signal is lost in the tail of the low-frequency phonon signal.

The leading edge of the second peak must be due to the creation of high-frequency phonons a few millimetres from the heater by interactions, because previous experiments have shown that no phonons with $\hbar\omega/k_B < 9.8$ K are detected as their mean free paths are so short [15, 19]. This is discussed more fully in section 3.5. So the true spectrum of high-frequency phonons arriving at the detector is narrower than the values presented at the beginning of this section, which were based upon a wholly ballistic path. Our evidence that these high-frequency phonons are not injected directly by the heater comes mainly from the dependence of the spectrum upon hydrostatic pressure.

3.3. Pressure dependence

As the hydrostatic pressure of the liquid ^{4}He is increased, the positive curvature of the low-frequency phonon dispersion curve decreases, and the threshold of stability against decay decreases from its value of $\hbar\omega_c^{(\infty)}/k_B = 10$ K at SVP until, for $P > 19$ bar, all phonons are stable [15, 11]. So, as the pressure is increased from SVP, it is reasonable to expect *a priori* the gap between the two phonon spectra to be gradually narrowed, but the number of $\hbar\omega/k_B > 10$ K phonons to be virtually unchanged. However, we find that the whole high-frequency phonon peak shifts closer to the low-frequency phonon signal, as can be seen in figure 5. So, for example, the number of $\hbar\omega/k_B = 10$ K phonons at $P = 5$ bar is less than the number of these phonons at 0 bar.

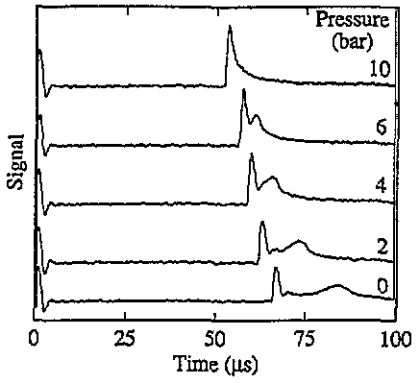

Figure 5. Signals at various hydrostatic pressures from a 0.1 μs, 10 mW mm^{-2} heater pulse. The signal path length is 15.7 mm, and $T < 0.1$ K. At 5 bar, we estimate from neutron scattering data [13] that 10 K phonons should arrive at $t \simeq 72$ μs. The oscillation on the tail of the first peak is an artefact of the detection system on this particular experimental run, as can be seen by the recovery from the electrical pick-up at $t < 5$ μs.

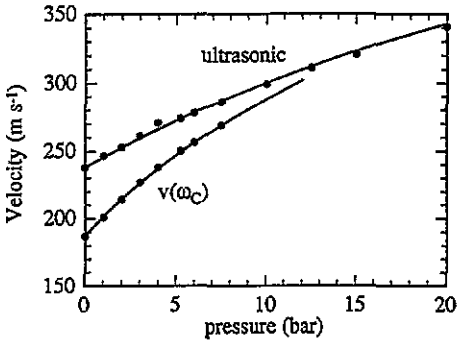

Figure 6. The velocities of the leading edge of the first peak and the maximum of the second peak of the signal as a function of pressure. The upper curve is a fit to published ultrasonic velocities [40], and the lower curve is a fit to the velocity of the decay cut-off as explained in the text.

The velocity of the low-frequency phonon peak as a function of pressure compares well with the published ultrasonic velocities [40], as shown in figure 6. This figure also shows that the velocity of the maximum of the second peak in the signal compares well with published estimates [9] of the phonon group velocity at the stability threshold $\omega_c^{(\infty)}(P)$, which were obtained from neutron scattering data and the assumption that

$$(\partial/\partial q)(\omega/q)|_{q_c} \tag{2}$$

varies linearly with pressure. We conclude that at each pressure P, the high-frequency phonon spectrum is strongly peaked around $\omega_c^{(\infty)}(P)$.

This pressure dependence excludes the possibility that these high-frequency phonons are injected directly by the heater and then propagate ballistically to the detector. Phonon processes in the heater and elastic transmission through the interface are unlikely to depend strongly upon pressure. Therefore the number of, say, $\hbar\omega/k_B = 10$ K phonons emitted by the heater via this channel would not significantly change as the pressure is increased. There should in fact be a small increase in direct phonon transmission due to the better sound velocity matching in the acoustic mismatch model, as opposed to the observed decrease in signal magnitude. The influence of pressure on the surface states responsible for inelastic transmission is not known, but this should only be important for the lower-frequency phonons emitted in this channel, and not for the high-frequency phonons observed in this experiment. We must therefore look to the scattering processes in the liquid as a source of our detected high-frequency phonons.

3.4. Previous evidence for phonon creation by scattering processes

The most reasonable explanation for the narrowness of the high-frequency phonon spectrum at this heater power (10 mW mm^{-2}) and its dependence upon pressure is that the detected high-frequency phonons are not emitted directly from the metal surface of the heater, but are created by scattering processes involving lower-frequency phonons in the liquid. In this case, it is unlikely that phonons with frequencies much higher than the decay cut-off are produced because the majority of phonons is of low frequency. The phonons are scattered up or decay down in energy until they reach $\omega_c^{(\infty)}$ whereupon they are relatively stable. They then escape from the interaction group by travelling more slowly than the low-frequency phonons. There is compelling experimental evidence that these interactions in the liquid do occur.

The creation of $\hbar\omega/k_B > 4.33$ K phonons by scattering in the bulk liquid has been demonstrated in an earlier experiment [41]. A number of parallel, closely spaced, one-dimensional heaters were pulsed separately or simultaneously. A pulse length of 1 μs and a relatively high power density of 25 mW mm^{-2} was used. The phonons were detected using an STJ with $2\Delta/k_B = 4.33$ K. When pulsed simultaneously, the detected signal was significantly greater than the sum of the signals from the individual heaters. This is evidence that frequency up scattering processes involving phonons from different heaters were occurring in the liquid.

So, for sufficiently high power densities ($W > 2$ mW mm^{-2}), interactions in the liquid create the majority of the high-frequency phonons that we detect as a signal peak.

3.5. Time of flight

We obtained a spectrum of high-frequency phonons from the observed signal by assuming that all the phonons are created at the heater surface and then travel ballistically to the

bolometer (figure 4). However, in the ballistic model, the leading edge of the signal is composed of phonon energies that should not be present due to spontaneous decays [15, 19]. The leading edge must therefore be composed of $\omega \simeq \omega_c^{(\infty)}$ phonons created by scattering processes in the liquid. Most of the high-frequency phonons are created close to the heater surface, thus giving the correct time for the signal maximum. Phonons arriving before the maximum appear to have been created from interactions between faster, lower-frequency phonons up to ~ 5 mm from the heater surface.

These creation processes provide an explanation for a long-standing problem with the time of arrival of quantum evaporation signals [31, 38]. The quantum evaporation of an atom by a phonon is a process in which energy and momentum parallel to the liquid surface are conserved. The model of this process gives a precisely determined time of flight for each phonon energy, assuming ballistic motion of the phonon between heater and liquid surface. Consequently, there exists a well defined minimum time of flight t_{min} for the complete range of phonon energies. These times were calculated using the dispersion curve measured by neutron scattering. Experiments have shown that the measured t_{min} is ~ 5 μs shorter than expected ($t_{min} \simeq 90$ μs for a path length of 6 mm in the liquid and 7 mm in the vapour) [31, 38, 39]. This discrepancy has now been observed in both quantum evaporation signals and direct phonon signals, and is due to high-frequency phonon creation at some distance from the heater surface. The evaporation experiments were performed using the same power and pulse width as used in these direct phonon experiments.

3.6. Temperature dependence

We have shown that the second peak in the observed signals is due to high-frequency phonons created by interactions amongst the injected phonons in the bulk liquid. The spectrum of these phonons is strongly peaked near $\hbar\omega/k_B \simeq 10.15$ K at SVP. These high-frequency phonons are stable against decay, but they will interact with the ambient thermal phonons in the liquid as they travel to the bolometer. This scattering rate increases with temperature as the energy and number density of the thermal phonons increases. We have modelled these interactions using the theory of four-phonon scattering. This model was developed to explain the attenuation of phonon evaporation signals [20].

In the computer model, monochromatic $\hbar\omega/k_B = 10.15$ K phonons are injected by the heater and their trajectories followed as they undergo four-phonon interactions until they either hit the bolometer or are lost from the signal. We use a monochromatic source in the model because we will be comparing the modelled attenuation with the dependence of the signal peak height upon liquid ^{4}He temperature. Since we believe that the phonons contributing to the signal maximum are ballistic from a point close to the heater surface, the time of flight discriminates for a narrow range of velocities, and hence phonon frequencies. Experiments have indicated short mean free paths for $\hbar\omega/k_B < 9.8$ K phonons [15, 19], so we assume in the model that any phonon with $\hbar\omega/k_B < 10$ K, i.e. $\omega < \omega_c^{(\infty)}$, is immediately lost from the signal due to spontaneous decay. If a high-frequency phonon is scattered to below $\omega_c^{(\infty)}$ near the bolometer, where time of flight can no longer discriminate between scattered and unscattered phonons, we can still discount the lower-frequency phonons because of the coefficient of energy transmission into the bolometer. When these $\hbar\omega/k_B < 10$ K phonons decay by cascade to lower-energy phonons, although the total energy arriving at the bolometer may be unchanged because of the small decay angles, the probability of transmission of this energy into the bolometer is much reduced due to its strong dependence upon phonon frequency for $\hbar\omega/k_B < 5$ K [3, 25]. Also, the model shows that a typical four-phonon interaction results in a large energy loss for the high-frequency phonon due mainly to the density of the final states, so that in the majority of cases, only

one interaction is needed to lose that phonon from the signal. This is supported by the observation that the signal shape does not change appreciably with liquid temperature; only its magnitude changes.

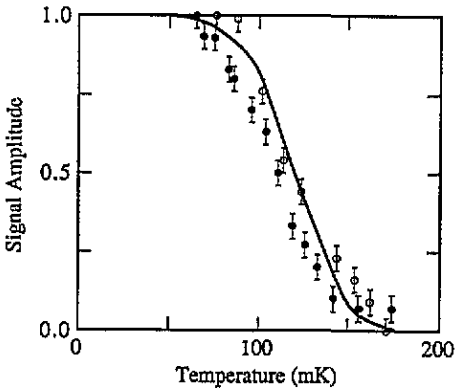

Figure 7. The magnitude of the high-frequency phonon signal (●) from a 0.2 μs, 10 mW mm^{-2} heater pulse as a function of liquid ^{4}He temperature at SVP. The path length is 15.7 mm. The curve is the modelled variation using four-phonon scattering theory. Also shown (○) for comparison are the evaporation signals from pulses of the same power and pulse width that traversed a liquid path length of 15.6 mm [20]. The curve and data are scaled to unity at the lowest temperature.

The signal magnitude as a function of temperature at SVP is plotted in figure 7 together with the results from the simulation. It shows the same trend as observed in the analysis of the attenuation of phonon evaporation signals with temperature. The experimental attenuation is only slightly greater than that predicted by the model. The small discrepancy may be due to the effect of the liquid thermal phonons on the creation mechanism for high-frequency phonons.

So, the temperature dependence of the high-frequency phonon signal can be modelled by taking into account the four-phonon interactions between these high-frequency phonons and the low-frequency ambient thermal phonons. We remind the reader that the model has no adjustable parameters.

4. Summary

We have succeeded in detecting the high-frequency phonon distribution created in liquid ^{4}He by a heated metal film using a bolometer submerged in the liquid. This is primarily due to optimizing the pulse length and power of the heater. The temporal separation of the high- and low-frequency distributions is clearly observed because of the velocity dispersion. The spectrum of high-frequency phonons is strongly peaked about the decay cut-off $\omega_c^{(\infty)}(P)$ at all pressures P up to at least 7.5 bar (which is the limit for resolving the maximum of this peak in the signal from the low-frequency phonon signal). The majority of these stable high-frequency phonons is created by interactions amongst the lower-frequency injected phonons in the bulk liquid. Most of the high-frequency phonons are created close to the heater surface, and then appear to travel ballistically to the detector. A few of the phonons are created up to ~ 5 mm from the heater surface. This explains the early time of

arrival of high-frequency phonons, which was first noticed in quantum evaporation signals. Increasing the liquid path length to a much greater distance would enable a more accurate spectrum of high-frequency phonons to be determined, but it would require low ambient liquid temperatures ($\ll$ 50 mK) to ensure that the mean free paths of the four-phonon interactions, involving the high-frequency phonons and the thermal phonons in the liquid, are longer than the signal path length. The attenuation of the high-frequency phonon signal with increasing liquid temperature is compared with a theoretical model of four-phonon interactions between the high-frequency phonons and thermal phonons in the liquid. Good agreement is found.

We have discovered a source of almost monoenergetic high-frequency phonons in liquid ^{4}He. The phonon frequency can, to some extent, be tuned by varying the liquid pressure.

References

[1] Atkins M and McClintock P V E 1976 *Cryogenics* **16** 733–4
[2] Maris H J 1977 *Rev. Mod. Phys.* **49** 341–59
[3] Challis L J 1974 *J. Phys. C: Solid State Phys.* **7** 481–95
[4] Wyatt A F G 1981 *Nonequilibrium Superconductivity, Phonons and Kapitza Boundaries* (New York: Plenum) ch 2
[5] Maris H J and Massey W E 1970 *Phys. Rev. Lett.* **25** 220–2
[6] Phillips N E, Waterfield C G and Hoffer J K 1970 *Phys. Rev. Lett.* **25** 1260–2
[7] Mills N G, Sherlock R A and Wyatt A F G 1974 *Phys. Rev. Lett.* **32** 978–81
[8] Dynes R C and Narayanamurti V 1974 *Phys. Rev. Lett.* **33** 1195–8
[9] Wyatt A F G, Lockerbie N A and Sherlock R A 1989 *J. Phys.: Condens. Matter* **1** 3507–22
[10] Stirling W 1983 *Proc. 75th Jubilee Conf. on ^{4}He* ed J G M Armitage (Singapore: World Scientific) p 109
[11] Jäckle J and Kerr K W 1974 *Phys. Rev.* A **9** 1757–9
[12] Svensson E C, Martel P and Woods A D B 1975 *Phys. Lett.* **55A** 151–2
[13] Stirling W 1985 private communication
[14] Greywall D S 1978 *Phys. Rev.* B **18** 2127–44
[15] Dynes R C and Narayanamurti V 1975 *Phys. Rev.* B **12** 1720–9
[16] Sluckin T J and Bowley R M 1974 *J. Phys. C: Solid State Phys.* **7** 1779–85
[17] Maris H J 1974 *Phys. Rev.* A **8** 1980–7
[18] Mezei F, Lartigue C and Farago B 1991 *Excitations in 2-Dimensional and 3-Dimensional Quantum Fluids (Exeter, 1990)* ed A F G Wyatt and H J Lauter (New York: Plenum) p 119
[19] Haavasoja T, Narayanamurti V and Chin M A 1984 *J. Low Temp. Phys.* **57** 55–9
[20] Tucker M A H and Wyatt A F G 1992 *J. Phys.: Condens. Matter* **4** 7745–58 Please note that one of the coefficients (c_7) in the parameterization of the dispersion curve was incorrectly given in this paper as positive. It should be negative, i.e. $c_7 = -0.0192$.
[21] Wyatt A F G, Sherlock R A and Allum D R 1982 *J. Phys. C: Solid State Phys.* **15** 1897–915
[22] Khalatnikov I M 1965 *An Introduction to the Theory of Superfluidity* (New York: Benjamin)
[23] Nothdurft E E and Luszczynski K 1978 *J. Physique Coll.* **39** C6 252–3
[24] Wyatt A F G and Page G J 1978 *J. Phys. C: Solid State Phys.* **11** 4927–44
[25] Bradshaw T and Wyatt A F G 1983 *J. Phys. C: Solid State Phys.* **16** 651–64
[26] Tucker M A H and Wyatt A F G 1994 *J. Phys.: Condens. Matter* **6** 2825–34
[27] Perrin N and Budd H 1972 *J. Physique Coll.* **33** C4 33–9
[28] Perrin N, Wybourne M N and Wigmore J K 1989 *Phys. Rev.* B **40** 8245–51
[29] Wyatt A F G 1989 *J. Phys.: Condens. Matter* **1** 8629–48
[30] Wyatt A F G and Brown M 1990 *Physica* B **165 & 166** 495–6
[31] Brown M and Wyatt A F G 1990 *J. Phys.: Condens. Matter* **2** 5025–46
[32] Guernsey R W and Luszczynski K 1971 *Phys. Rev.* A **3** 1052–9
[33] Pfeifer C D and Luszczynski K 1973 *Phys. Rev.* A **7** 1055–61
[34] Chrome and titanium films supplied by Dr N Mulders
[35] Supplied by Lake Shore Cryotronics, OH, USA
[36] Supplied by Lancaster University
[37] Sherlock R A and Wyatt A F G 1983 *J. Phys. E: Sci. Instrum.* **16** 669–82

[38] Tucker M A H and Wyatt A F G 1990 *Physica* B **165 & 166** 493–4
[39] Forbes A C and Wyatt A F G to be published
[40] Maynard J 1976 *Phys. Rev.* B **14** 3868–91
[41] Korczynskyj Y and Wyatt A F G 1978 *J. Physique Coll.* **39** C6 230–1